

Integrated model for the prediction of cleaning profiles inside an automatic dishwasher

Pérez-mohedano, R.; Letzelter, N.; Bakalis, S.

DOI:

[10.1016/j.jfoodeng.2016.09.031](https://doi.org/10.1016/j.jfoodeng.2016.09.031)

License:

Creative Commons: Attribution-NonCommercial-NoDerivs (CC BY-NC-ND)

Document Version

Peer reviewed version

Citation for published version (Harvard):

Pérez-mohedano, R, Letzelter, N & Bakalis, S 2017, 'Integrated model for the prediction of cleaning profiles inside an automatic dishwasher', *Journal of Food Engineering*, vol. 196, pp. 101-112.
<https://doi.org/10.1016/j.jfoodeng.2016.09.031>

[Link to publication on Research at Birmingham portal](#)

Publisher Rights Statement:

Checked 14.11.2016

General rights

Unless a licence is specified above, all rights (including copyright and moral rights) in this document are retained by the authors and/or the copyright holders. The express permission of the copyright holder must be obtained for any use of this material other than for purposes permitted by law.

- Users may freely distribute the URL that is used to identify this publication.
- Users may download and/or print one copy of the publication from the University of Birmingham research portal for the purpose of private study or non-commercial research.
- User may use extracts from the document in line with the concept of 'fair dealing' under the Copyright, Designs and Patents Act 1988 (?)
- Users may not further distribute the material nor use it for the purposes of commercial gain.

Where a licence is displayed above, please note the terms and conditions of the licence govern your use of this document.

When citing, please reference the published version.

Take down policy

While the University of Birmingham exercises care and attention in making items available there are rare occasions when an item has been uploaded in error or has been deemed to be commercially or otherwise sensitive.

If you believe that this is the case for this document, please contact UBIRA@lists.bham.ac.uk providing details and we will remove access to the work immediately and investigate.

Accepted Manuscript

Integrated model for the prediction of cleaning profiles inside an automatic dishwasher

R. Pérez-Mohedano, N. Letzelter, S. Bakalis



PII: S0260-8774(16)30360-0
DOI: [10.1016/j.jfoodeng.2016.09.031](https://doi.org/10.1016/j.jfoodeng.2016.09.031)
Reference: JFOE 8676
To appear in: *Journal of Food Engineering*
Received Date: 22 June 2016
Revised Date: 04 September 2016
Accepted Date: 28 September 2016

Please cite this article as: R. Pérez-Mohedano, N. Letzelter, S. Bakalis, Integrated model for the prediction of cleaning profiles inside an automatic dishwasher, *Journal of Food Engineering* (2016), doi: 10.1016/j.jfoodeng.2016.09.031

This is a PDF file of an unedited manuscript that has been accepted for publication. As a service to our customers we are providing this early version of the manuscript. The manuscript will undergo copyediting, typesetting, and review of the resulting proof before it is published in its final form. Please note that during the production process errors may be discovered which could affect the content, and all legal disclaimers that apply to the journal pertain.

- An integrated model to predict cleaning profiles inside an automatic dishwasher is proposed.
- Water jets trajectories are evaluated via a mathematical model based on geometry principles.
- Kinetics of soil removal are evaluated using a fluid dynamic gauge.
- Mechanisms of removal are combined and integrated together to simulate removal data.
- Validation is done by comparison with real data.

Integrated model for the prediction of cleaning profiles inside an automatic dishwasher

R.Pérez-Mohedano^{a,b}, N.Letzelter^b, S.Bakalis^a

^a Centre for Formulation Engineering, Department of Chemical Engineering, University of Birmingham, Edgbaston, Birmingham B15 2TT, UK

^b Procter & Gamble Innovation Centers Ltd., Whitley Road, Longbenton, Newcastle Upon Tyne, NE12 9TS, UK

1. Introduction

There are a number of consumer operations, including automatic dishwashers (ADWs), where chemical engineering approaches could help overcome the current semi-empirical approach. A typical ADW cleaning cycle consists of a series of rinse and main wash stages in which the detergent is released from its compartment and temperatures are varying during the length of the cycle. A great performance would involve the complete cleaning and drying of a wide variety of items in the least time possible and consuming low amounts of water and energy. Significant savings in water consumption (~75%) and energy used (~25%) are currently achieved when compared with the hand washing of a standardised load (Berkholz et al., 2010). The result is influenced by the water coverage and physical energy input (which depends on the appliance design), the distribution of items (partially user-dependant) and the performance of the formulated detergent used.

The coverage produced by the water jets is believed to be a key factor for the effectiveness of cleaning (Wang *et al.*, 2013a). Within ADWs, impinging jets may impact the different surfaces at a wide range of angles. Different angles of ejection are obtained by varying the design of the individual nozzles present in a spray arm and by changing the pump pressure. This produces different ejection paths depending on the nozzle considered. Also, the spray arm rotation rate is a consequence of the total torque generated. Generally, the presence of one or more 'driving nozzles' at the bottom of a spray arm creates a net force due to the reaction force that is produced on the spray arm once the water is ejected (Newton's third law).

Current detergent formulations encompass a wide range of ingredients (Tomlinson and Carnali, 2007). They can be grouped according to the role they play during a wash cycle. *Buffers* are required to maintain pH, influencing the swelling and gelification phenomena needed for the successful removal of protein and starch-based soils. *Builders and antiscalants* control the water hardness and avoid the formation of undesired precipitates on glassware. *Bleaches* aim to perform a germicidal action and to remove stains like tea. Surfactants are required to control foaming and to increase the wettability of the different items. An excessive foaming would cause a malfunction of the spray arms due to the displacement of bubbles to the pumps, therefore surfactants added to ADW formulations typically perform an antifoaming or defoaming action. Finally, enzymes are one of the key ingredients across automatic dishwashing industry nowadays (Aehle, 2007; Olsen and Falholt, 1998). The low levels set in formulation made possible their inclusion in commercial detergents. *Enzymes* help the reduction of wash times, lower the required pH and provide a more environmentally friendly effluent. Two major groups of enzymes are used: proteases and amylases. They must perform correctly in a wide range of temperatures (20°C to 70°C) and with an optimum temperature performance around 60°C; show high activity at basic conditions; be stable in the presence of other detergent ingredients; and target a wide variety of soils.

Small-scale techniques of increasing complexity have been developed throughout the years to better understand cleaning both in the context of ADWs as well as industrial Cleaning-In-Place processes (CIP) (Wilson, 2005). A *flow channel*, developed by (Christian and Fryer, 2006), flows a wash solution upon a soil sample attached to a substrate while enabling the evaluation of cleaning via image analysis, pressure drop and heat transfer coefficient changes. The reported technique has been used to study removal of different fouling materials, such as, yeast (Goode et al., 2010), toothpaste (Cole et al., 2010), sweetened condensed milk (Othman et al., 2010), or whey proteins (Christian and Fryer, 2006), under different cleaning times and Re numbers that were correlated to wall shear stress. A *micromanipulation* rig was developed to measure the energy required to remove adhesive and cohesive deposits from different surfaces (Liu et al., 2002). Different analyses on multiple soils (i.e tomato paste, egg albumin, whey protein concentrate, milk protein or bread dough) have also been reported (Liu et al., 2006a, 2006b, 2006c, 2005). A similar system, called *millimanipulation*, has been recently developed by Ali et

al., (2015) to study highly adhesive soils, such as baked lard. *Fluid Dynamic Gauging (FDG)* also allows to explore indirectly the behaviour of soft soil deposits by measuring the thickness evolution when submerged in a liquid environment (Gordon et al., 2010a, 2010b; Tuladhar et al., 2000, 2002). Finally, the impact of *impinging jets* at different angles over a flat surface and their correlation to the effectiveness of cleaning has also been investigated (Wang et al., 2014, 2013a, 2013b; Wilson et al., 2014, 2012). These various techniques have aided to an improved understanding of the mechanisms of soil removal. However, current industry standardised ADW cleaning tests only evaluate the performance of an appliance or detergent once the cleaning cycle is finished (AHAM, 1992). Technical items are evaluated using a visual method before and after the wash cycle and not during it. Timescale is not considered. Therefore, the introduction of time as a factor and the necessity of understanding the limitations and interactions of mechanical and chemical components throughout the wash cycle become essential.

Moreover, cleaning of highly attached dry deposits is complex. Particularly, egg yolk soils are one of the most challenging. This material is highly difficult to remove from a hard surface when dried and is one of the typical consumer complaints within the automatic dishwasher industry (DuPont, 2012). Three stages can be identified in the cleaning process (Bird and Fryer, 1991): 1) an *initial swelling* when the soil and the wash solution are put into contact; 2) a *constant removal rate* once the removal of the substance occurs and 3) a final *decay* of the removal rate when adhesive forces become important.

The present paper aims to address the link between mechanical and chemical processes occurring over time in a typical dishwasher operation. For that, this work presents the combination of methods and models to predict phenomena occurring at the scale of an actual automatic dishwasher and more specifically to predict the cleaning path of a typical hard-to-remove soil. For the presented system, only buffers and enzymes are studied as key ingredients within current commercial formula.

2. Methodology

To provide an integrated model solution, it is necessary to simulate both the flow of water inside the appliance as well as the behaviour of the soil at the different cleaning conditions established. Water flow depends on the specific design of the ADW and the distribution of items inside it, while the cleaning evolution is also a function of the status of the soil sample (i.e. moisture content) and the mechanical and chemical conditions set. The different phenomena must be combined and integrated over time to predict the cleaning evolution of a typical soil. Finally, a comparison against experimental data is necessary to validate the model solution proposed. **Figure 1** shows a schematic representation of the methodology followed.

This work develops three main areas to provide an integrated model:

- 1) *Mathematical model for the prediction of water jets trajectories based on dishwasher design:* an analysis on the water motion inside an ADW using Positron Emission Particle Tracking (PEPT) already reported that the initial distribution of water in current ADWs occurs via coherent jets from the different nozzles in the spray arms (Pérez-Mohedano et al., 2015a). From a particular position a jet follows a defined trajectory that can be estimated by using geometric principles. A mathematical model which predicts the jet trajectory and impact points according to the nozzle and spray arm design and the position of the item to be cleaned is developed in consequence.
- 2) *Small-scale statistical models for the various cleaning mechanisms identified on protein cleaning:* the cleaning sequence followed by a typical dry egg yolk sample consists of an initial swelling stage followed by a removal phase which could occur via soil dissolution (enzymatic-induced removal) or removal via shear stress action (mechanical and enzymatic-induced removal) (Pérez-Mohedano et al., 2015b). Additionally, removal mechanisms showed an initial transition period with none or negligible removal followed by a steady increase to a constant value after a certain time. To collect data regarding the removal mechanisms and lag time, a custom design set of experiments using scanning Fluid Dynamic Gauging (sFDG) is presented in this work. **For swelling**

phenomenon it was required a diffusion coefficient (D), Flory-Huggins parameter (X), number of polymer chains per unit volume (N), the volume of a solvent molecule (water) (Ω) and the thickness at equilibrium (h_{\max}), whose values can be originally found in Pérez-Mohedano et al., (2016) and are summarised further in **Table 5**. Data from each individual mechanism is analysed separately and modelled according to different statistical procedures.

3) *Integration of the individual models developed and comparison of the simulations performed with real data for validation purposes:* to integrate the swelling and removal behaviour of protein-based soils explained above, an algorithm was reported (Pérez-Mohedano et al., 2015b) and summarised in **Eq. 1**:

$$\frac{dh}{dt} = S - f \cdot SS - (1 - f) \cdot SD \quad \text{Eq. 1}$$

Where:

- h = Thickness of the soil sample.
- t = Time.
- S = Swelling function.
- SS = Shear Stress function.
- SD = Soil Dissolution function.
- f = Frequency function. Step function (0 or 1).

Thickness change of a soil sample over time is a function of the swelling (positive thickness variation) and removal either by shear stress action or soil dissolution (negative thickness variation). The frequency function accounts for the periods when an external mechanical action is being applied on the sample or not. It is a step function with a value of 0 when no external mechanical action occurs and a value of 1 when it does. This cancels the term not applicable at each specific time. The integration of the equation allows to represent the evolution of the soil thickness at varying cleaning conditions.

In this work, data from the mathematical model on jets trajectories is used to determine the frequency (f) of impact of the different jets generated in the ADW. This information is then combined with individual statistical models for the various cleaning mechanisms (swelling (S), shear stress (SS) and soil dissolution removal (SD)) as a function of the conditions in the ADW: temperature, pH, enzyme level, shear stress and frequency factor.

To generate real data, an image analysis system was designed to evaluate cleaning in ADW in real time. Results are finally compared with simulations performed from the swelling-removal algorithm.

3. Materials & Experimental Procedure

3.1. Soil Technical Samples

Egg yolk samples were used as the soil type to study. It is a complex mixture with a typical dry composition of approximately 62.5% fats, 33% proteins, 3.5% minerals and 1% of carbohydrates (Mine and Zhang, 2013). Its main structure is formed by high (HDLs) and low density lipoproteins (LDLs) in the shape of spheres that surround a lipid core. Despite the larger proportion of fats, the samples are considered protein-based as their properties depend precisely on their protein network. For example, its behaviour follows the typical cleaning sequence of protein concentrated deposits (Fryer et al., 2006). Also, at above 70°C, egg yolk samples have been reported to form protein aggregates able to swell due to their amphiphilic properties (Denmat et al., 1999; Tsutsui, 1988). These behaviours were observed with the samples used in this work, thus it was maintain their reference as protein-based soils.

The tiles were purchased from Centre For Testmaterials (CFT, products DS-22 / DM-22, C.F.T. BV, Vlaardingen, the Netherlands). They were made by spraying layers of egg yolk over a stainless steel or melamine base. Specifics on the preparation of the samples remained unknown due to confidentiality reasons from the samples' manufacturer. Stainless steel substrates were used for scanning fluid dynamic gauge experiments as a completely flat and non-swellable surface was needed. Melamine substrates were used in tests in the ADW unit due to the white background required for colour measurements. Samples were kept in a fridge at temperatures below 5°C until their usage for their correct preservation. Original size of the tiles used was 12

cm x 10 cm. However, melamine tiles were cut to 6cm x 10cm, corresponding to half of the original purchased size. Their initial thickness and mass were 68 μm ($\pm 14 \mu\text{m}$) and 1.75 g (± 0.04 g) with a water content of 0.11 grams (± 0.03 g) for their original size.

3.2. Research techniques

3.2.1. Automatic Dishwasher Unit

Experiments performed inside an automatic dishwasher (ADW) were carried out in a customised Whirlpool unit (DU750 model). The appliance was programmed to run at two constant washing temperatures (30°C and 55°C) with only the lower spray arm ejecting water and at a rotation rate of 35 rpm. The length of the cycles was up to 2 hours without any initial or final rinse stage.

3.2.2. Camera kit

A waterproof camera was the tool used to gather online images through the wash cycle. A waterproof torch with good resistance to high temperatures was also used as the light source inside the ADW. Specific details on the design and set-up of the camera kit have been intentionally avoided to preserve its confidentiality. The system aimed to evaluate the cleaning evolution of technical CFT tiles via color changes.

3.2.3. Scanning Fluid Dynamic Gauge

Scanning Fluid Dynamic Gauge (sFDG) was the technique selected for the analysis of the cleaning evolution of technical protein samples in a small-scale and controlled environment. It allows to measure thickness changes on immobile flat samples. A gauging fluid is passed through a nozzle and its flow is gravity-maintained. Any changes in the sample as a consequence of its swelling or removal varies the flow. To keep it constant, the nozzle must move up or downwards to adapt to the situation. These movements are recorded through a data logger to a computer and then translated into the thickness of the sample at different experimental times. A wide range of conditions can be controlled and study: temperature, chemistry (pH, enzyme concentration, ionic strength...), shear stress and frequency of application of shear stress over various locations on the sample.

3.3. Experimental procedure

3.3.1. sFDG tests – Individual statistical models

To develop the individual statistical models for the two mechanisms of removal (soil dissolution and shear stress) and the 'lag time' prediction, a 22 experiments custom-design was established in the sFDG. Swelling data was collected in a recently published study (Pérez-Mohedano et al., 2016) and can be observed in Table 5. Temperature and pH were in a range from 30 °C to 55 °C and 9.5 to 11.5 respectively. Enzyme levels were set between 0.02 g/l and 0.10 g/l. These ranges are the ones typically set in ADW cleaning cycles. Enzymes used were specific proteases designed for its use in ADWs. Shear stress imposed was established from 12 Pa to 65 Pa, matching the lowest and highest shear stress exerted by the gauging fluid. Frequency factor ranged from 8.5% to 100%. A frequency factor of 8.5% was set by tracking 6 different locations per sample. As the gauging nozzle needed time to move from one location to another, the imposition of external shear stress lasted approximately 30 seconds per location. The scanning sequence was repeated every 6 minutes. A frequency factor of 100% means that the nozzle was sited over a single location for the duration of the experiment.

The initial water hardness was established at 8.5 US gpg (4.4 mM) by maintaining a molar ratio between $\text{CaCl}_2 \cdot 6\text{H}_2\text{O}$ and $\text{MgCl}_2 \cdot 6\text{H}_2\text{O}$ of 3:1. 0.236 g/l of $\text{CaCl}_2 \cdot 6\text{H}_2\text{O}$ and 0.076 g/l of $\text{MgCl}_2 \cdot 6\text{H}_2\text{O}$ were added to the deionised water used. pH was established and maintained via buffer solutions. It was measured with a pH meter (product Orion 4 Star™, Thermo Scientific Orion). The different pH were achieved as follows:

- For pH 9.5, 0.112 g/l of Na_2CO_3 and 0.150 g/l of NaHCO_3 were used ($[\text{Na}_2\text{CO}_3] = 1.10 \text{ mM}$ and $[\text{NaHCO}_3] = 1.80 \text{ mM}$).
- For pH 10.5, 0.106 g/l of Na_2CO_3 were added ($[\text{Na}_2\text{CO}_3] = 1.00 \text{ mM}$).
- For pH 11.5, 0.13 g/l of NaOH were added ($[\text{NaOH}] = 3.25 \text{ mM}$).

Chemicals were added and recirculated through the system 10 minutes prior the start of the tests. Temperatures were monitored with the aid of waterproof digital thermometers. More details on the specifics in the use of the sFDG and the data processing can be found in Pérez-Mohedano et al., (2015b).

Table 1 summarises the experimental approach already taken for swelling data and the approach presented in this paper to model removal mechanisms, which experimental matrix is shown in **Table 2**.

Table 1. Summary of the two different Design of Experiments considered.

MODEL	FACTORS	RANGE CONSIDERED	TYPE OF DESIGN
Swelling (No enzymes)	<i>Temperature</i>	30°C – 55°C	Full Factorial (9 experiments) Data found in Pérez-Mohedano et al., (2016)
	<i>pH</i>	9.5 – 11.5	
Swelling + Removal (With enzymes)	<i>Temperature</i>	30°C – 55°C	Custom design (22 experiments) Data found in Table 2 .
	<i>pH</i>	9.5 – 11.5	
	<i>Enzyme</i>	0.02 g/l – 0.10 g/l	
	<i>Shear Frequency</i>	8.5% - 100%	
	<i>Shear Stress</i>	12 Pa – 65 Pa	

Table 2. Experiment matrix for the 22 experiments custom design in the sFDG.

#	T (°C)	pH	ENZYME (g/l)	FREQUENCY FACTOR (%)	SHEAR STRESS (Pa)
1	55	9.5	0.10	9	65
2	30	9.5	0.06	54.5	65
3	30	10.5	0.02	9	38.5
4	55	11.5	0.02	100	12
5	30	9.5	0.10	9	12
6	42.5	10.5	0.06	54.5	38.5
7	30	11.5	0.06	54.5	38.5
8	55	9.5	0.06	9	12
9	42.5	9.5	0.02	54.5	38.5
10	30	9.5	0.10	100	38.5
11	55	9.5	0.02	100	65
12	42.5	11.5	0.10	100	12
13	30	10.5	0.10	54.5	65
14	42.5	10.5	0.06	100	38.5
15	30	10.5	0.02	100	12
16	55	11.5	0.10	9	38.5
17	55	10.5	0.02	54.5	65
18	55	11.5	0.10	100	65
19	42.5	11.5	0.06	9	65
20	55	9.5	0.10	54.5	12

21	30	11.5	0.02	100	65
22	42.5	11.5	0.02	9	12

3.3.2. ADW tests

ADW tests generated the information required to compare the integrated model with real data. Experiments studied temperature, pH and enzyme level effects in a real wash environment. Shear stress applied and frequency factor remained constant as they were dependent on the appliance design and spray arm rotation rate which were invariant. **Table 3** summarises the 6 different wash conditions run:

Table 3. Summary of the six different ADW experiments considered.

EXPERIMENT	TEMPERATURE	pH	ENZYME LEVEL
1	30°C	10.5	0.06 g/l
2	55°C	10.5	0.06 g/l
3	55°C	10.5	0.02 g/l
4	55°C	10.5	0.10 g/l
5	55°C	9.5	0.06 g/l
6	55°C	11.5	0.06 g/l

Deionised inlet water was preheated in an external tank at the desired temperature so no extra heating effort from the dishwasher was needed. The water hardness was initially established at 8.5 US gpg (4.4 mM) by following the same procedure as for sFDG tests. Chemistry required was added at the bulk water at the bottom once the dishwasher finished filling it up. Chemicals were mixed during 5 minutes before the camera, torch and CFT tile were placed internally. Test were performed with no items loaded except the camera kit and soil sample, which were placed in at the back-left side of the lower basket. Pictures were taken every 5 seconds and information collected until the camera shut down (typically 65-70 minutes, 1300-1400 images). Triplicates were done for each experimental condition considered. Once a experiment was completed, images were loaded to a computer for further processing. **Figure 2** illustrates a schematic of the set-up of the camera kit inside the ADW.

3.4. Data analysis

3.4.1. sFDG tests - Individual statistical models

Statistical analyses were carried out by using JMP® software (v. Pro 11.1.1). Partial Least Squares (PLS) was the initial method selected to analyse output data from the scanning Fluid Dynamic Gauge. This technique is a regression method typically more robust than classical principal components approaches (Geladi and Kowalski, 1986). In order to gain a better insight on the method development and principles, the reader is referred to Wold (1985). The technique, rather than single outputs, enables the processing of time-evolving results.

To discretise and normalise each effect studied along the different time responses obtained, JMP software allows to build *Normalised Effect Plots*. These plots represent the significance of each factor over time. Values are normalised between -1 to +1. A negative value indicates a negative effect on the response while a positive value indicates the opposite. The closer the value to -1 or +1, the higher the influence of a factor at that time.

Once sFDG data was initially analysed via PLS methodology, soil dissolution, shear stress removal rates and lag times were estimated for each individual experiment. Values were calculated by integrating the experimental slopes found in raw data for the different mechanisms occurring (Pérez-Mohedano et al., 2015b). With that information, Response Surface (RS) models (Bezerra et al., 2008) were built to estimate removal rates and lag times as a function of the factors studied: temperature, pH, enzyme, frequency factor and shear stress applied.

3.4.2. ADW tests - Image processing

A customised software was used to analyse the pictures taken during an ADW test. Images were evaluated by transforming their initial RGB colour values into L*a*b ones (Jin and Li, 2007). Colour contrasts between the background white colour shown on the melamine substrate and images taken at different times were estimated. A Stain Removal Index (SRI) was defined as expressed in Eq. 2 (Neiditch et al., 1980). The definition established a range of values between 0 and 100. A value of 0 indicates no cleaning (or colour change) when compared to the initial soiled tile. A value of 100 indicates a complete cleaning or complete colour matching with the background

white colour. The representation of SRI values over time allowed the visualization of the cleaning kinetics. The slope of the curve represents the removal rate at every time (i.e. %/min).

$$SRI (\%) = \frac{(Contrast)_{t=0} - (Contrast)_{t=t}}{(Contrast)_{t=0}} \cdot 100 \quad \text{Eq. 2}$$

Where:

$$(Contrast)_{t=0} = \sqrt{(L_{t=0} - L_{white})^2 + (a_{t=0} - a_{white})^2 + (b_{t=0} - b_{white})^2} \quad \text{Eq. 3}$$

$$(Contrast)_{t=t} = \sqrt{(L_{t=t} - L_{white})^2 + (a_{t=t} - a_{white})^2 + (b_{t=t} - b_{white})^2} \quad \text{Eq. 4}$$

4. Results & Discussion

4.1. Mathematical model for the prediction of water jets trajectories

4.1.1. Assumptions

The model considers that the initial distribution of water around the inner volume of the dishwasher occurs via coherent jets formed as the water goes through the different nozzles (Pérez-Mohedano et al., 2015a). The subsequent spread of water via breakage of those jets after impacting different surfaces and the waterfall created in some areas is not considered here due to the significant complexity that arises. The methodology attempts to evaluate only the distribution of water until the impact of those jets.

Impacts are studied as the intersection projection of a jet over the plane generated by the analysed item. As coherent jets are assumed (negligible changes on their diameter once ejected and no breakage of them), a single impact point occurs from a defined nozzle position and spray arm location in the ADW. As the spray arm rotate, the nozzle position varies and more impact points are defined.

4.1.2. Definition of variables

The paths of the jets produced from different nozzles are characterised by a direction vector. This indicates the 3D trajectory the coherent jet will follow and it can be expressed in polar coordinates. An angle theta (θ_{jet}) is defined as the angle the jet has in the x-y plane (plan view). Another angle, rho (ρ_{jet}), is defined as the angle between the x-y plane and z-axis (front view). The combination of both gives the 3D projection that describes the trajectory of the jet. **Figure 3** illustrates a visual representation of the parameters defined.

The space between the soiled item and the previous item sitting in front of it (i.e. two plates loaded one in front of each other) must also be considered. This space is named as '**vision area**'. It is assumed that any nozzle standing out of the **vision area** will not hit the soiled item as the item in front will block the jet trajectory coming from that nozzle. The time a nozzle is travelling within that vision area (t_{vis}) per spray arm rotation represents the maximum time a jet is likely to impact the soiled item. As the trajectory of a nozzle travelling within that area is circular, t_{vis} is a function of the angular positions at which the nozzle enters (β_{in}) and exits (β_{out}) the defined 'vision area' and the rotational speed of the spray arm (ω). Different radial nozzle positions in the spray arm also influence the available time a nozzle is travelling within the vision area (t_{vis}). The closer the nozzle to the axis of rotation the longer the time travelling in that area. This is a consequence of the symmetry between items placed in parallel and the rotational movement of the spray arm. In **Figure 4**, the angle displacement for two nozzles at different radial positions is proved to be different when symmetry between items exists ($\beta_1 > \beta_2$). As the angular velocity ($\omega = \frac{d\beta}{dt}$) is the same and the angle covered different, t_{vis} is therefore different between nozzle #1 and #2. Higher separation between items also provides longer times in the vision area. A displacement of the soiled item towards the front or back of the dishwasher also changes the radius distance where the item is located from the origin. Thus, angles and time in vision area also vary.

Two parameters are defined as outputs: the total time a jet is directly impacting the soiled item per rotation (T_{impact}) and the length (L_{impact}) covered by the impact. To see in detail the mathematical approach to calculate them, the reader is referred to the *Appendix* section.

4.1.3. Water trajectories for ADW tests

Given the set-up considered, the required input parameters to estimate T_{impact} and L_{impact} are: the coordinates of the area occupied by the tile, the 'vision area' distance, the spray arm rotation rate and the design parameters of the different nozzles in the lower spray arm. Both the coordinates of the soil tile (see **Figure 2**) and the rotation of the spray arm (35 rpm or 1.71 seconds per revolution) have been already commented. As *vision area* it was considered the space between the soil tile and the camera. This distance was set at 75 mm. Out of the 10 nozzles available in the lower spray arm, the model predicted only two able to directly impact the CFT tile. The others were designed in a way that either hit the backside of the tile or did not hit the tile at all at its location in the ADW. The design characteristics of the two nozzles are shown in **Table 4**. The values of the estimated outputs are also available in that table.

Table 4. Input and output values for the full-scale set-up.

#	NOZZLE POSITION (R_{NZ} [=] mm)	THETA ANGLE (θ_{jet} [=] degrees)	RHO ANGLE (ρ_{jet} [=] degrees)	t_{vis} (s)	T_{impact} (s)	L_{impact} (mm)
1	226	359	89	0.096	0.0013	59.9
2	145	305	70	0.169	0.027	60.9

For jet #1, the impact time over the tile was estimated at 0.0013 seconds per revolution of the spray arm. This corresponds to only 0.07% of the total rotational time. This is a consequence of the rho angle design value ($\rho_{\text{jet}} = 89$ degrees), which projects the jet almost vertically in the dishwasher. For jet #2, the impact time was higher and estimated to be 0.0272 seconds. This led to a frequency of impact of 1.59% of the total rotational time. The rho angle design ($\rho_{\text{jet}} = 70$ degrees) projected this jet less vertically in the dishwasher, thus allowing it to impact the soil tile for longer. For the integrated model simulations, the frequency of application of an external shear stress over the soil tile was assigned a value of 1.59%, representing the best-case scenario

estimated. It was also assumed that the shear stress generated across the CFT tile area was homogeneous at any time the impact of the jets occurred.

4.2. Statistical models for the prediction of individual cleaning mechanisms rates

4.2.1. Partial Least Squares analysis

An initial PLS analysis to the data generated via the 22 custom-design experiments determined that, among the factors considered, temperature, pH, enzyme level and the frequency factor were significant contributors to the thickness change of the egg yolk CFT tiles. However, the net shear stress applied over the sample did not produce a significant impact on thickness change within the range studied (from 12 to 65 Pa). This indicates that the removal of soil layers occurred faster whenever some external energy input was applied (frequency factor), but that an increase in the external energy imposed (net shear stress) barely changed the rate of removal. **Figure 5** shows a normalised effect plot that describes the effect on thickness over time for each of the main factors studied. A negative value indicates a negative effect on thickness (removal) while a positive value indicates the opposite (swelling).

Temperature (blue line) showed an initial positive contribution to thickness during the first 20 minutes, corresponding to the swelling stage. At around 20 minutes, the transition from a net swelling stage (net increase in thickness) to a removal phase (net decrease in thickness) was typically seen experimentally. At longer times, temperature contribution shifted from a positive to a negative effect on thickness with an increasing importance over time. **Despite its effect was higher at the removal stage (peak at -0.6) than at the swelling stage (peak at 0.4), no successful removal could occur without an initial swelling, where thermal and diffusional processes are dominating. The plot also expresses that once removal starts to occur the importance of temperature increases at longer times in comparison with the rest of factors.** Overall, it can be concluded that temperature is a net contributing factor for all the phenomena occurring in a typical protein-based cleaning process. **A higher temperature would translate into a better performance.**

pH (red line) was highlighted as a very important factor during the swelling stage of the process. The plot shows how pH influences thickness at early times (i.e. at 10 minutes) with a normalised

maximum value around 0.9. Its contribution decreased afterwards in parallel with a reduction of the swelling rate as the stretch of the soil network approximated the equilibrium. At that stage removal mechanisms became predominant. The plot illustrates as well the negligible contributions of pH to removal. Low negative values are seen after 60 minutes, when tiles were almost or completely cleaned. This result indicates that high alkalinity is required at the first stages of a protein-based soil cleaning process. However, alkalinity is not an important factor once removal occurs.

The effect of the *enzyme* (green line) became significant after an initial lag period of approximately 10 minutes. As a protease enhances soil hydrolysis and increase washing performance, its effect on thickness was negative. After the initial lag time, the enzyme showed an increased negative effect on thickness until the lowest value was found at around 30 minutes (peak at -0.5). The enzyme was the main contributor to removal and its effect varied slowly once the peak was achieved, remaining almost invariant during most of the removal process (from 20 minutes to 80 minutes).

The frequency of application of shear stress over the soil (purple line) was also an important contributor to removal, following a similar trend as for the enzyme. However, during the initial swelling stage it showed a positive effect on thickness. This suggests that the application of an external shear stress and the water suction produced through the sFDG nozzle could enhance the diffusion process occurring. After that period, the effect shifted to a negative contribution. Its peak was found at around 30 minutes with a normalised effect value around -0.5. It can be concluded that both the frequency factor and enzyme level were the main contributors to cleaning for this particular soil.

Finally, net shear stress effect (orange line) remained barely flat over time. This indicates, as already commented, the negligible effect of increasing the mechanical energy action within the range studied.

Similar conclusions were extracted from previously reported work by Gordon et al., (2012) on protein-based soils using the sFDG,

4.2.2. Response surface models

Figure 6 illustrates the actual by predicted plots for each statistical model built for the soil dissolution and shear stress removal mechanisms and the lag time. R^2 and R^2 adjusted values are also shown.

For *soil dissolution removal rate* model, input factors considered were the individual response surfaces of temperature (e.g. RS*Temperature), pH and enzyme level, their interactions (e.g. pH*enzyme) and square terms (e.g. pH*pH). As this removal phenomenon is not related to the application of any external mechanical action, the frequency factor and shear stress applied were not incorporated as inputs. *Shear stress removal rate* model built used as input factors the individual response surfaces of temperature, pH, enzyme level and frequency factor, and their second polynomial to degree interactions (i.e. temperature*temperature, temperature*pH, temperature*enzyme, temperature*frequency for temperature factor). Shear stress was not incorporated as a factor as the statistical analysis in the previous section did not highlight this parameter as significant in the swelling-removal process. Finally, *lag time model* used as input factors the individual temperature, pH, enzyme level and frequency factor response surfaces (e.g. temperature*RS) and their square terms.

Overall, models built showed relatively high agreement with real data ($R^2 > 0.84$). Bigger deviations were expected at the extreme values (i.e. large lag times or high soil dissolution or shear stress removal rates), as the number of data points was lower.

With all these tools already presented and data shown, it was possible to estimate ADW cleaning profiles at the different experimental conditions shown in **Table 3**.

4.3. Integrated simulation and comparison with real data.

Figure 7 illustrates the comparisons made between real and simulated data for the ADW tests. **Table 5** indicates the experimental conditions for each case as well as the simulation parameters used to develop cleaning profiles based on **Eq. 1**. Swelling phenomenon required data that were previously estimated in Pérez-Mohedano et al., (2016). Lag times, shear stress and soil

dissolution removal rates were also estimated for each case by applying the statistical models developed in this work.

485

486 **Table 5.** Input and output values for the ADW integrated model.

EXPERIMENTAL CASE		1	2	3	4	5	6
EXPERIMENTAL CONDITIONS							
Temperature		30°C	55°C	55°C	55°C	55°C	55°C
pH		10.5	10.5	10.5	10.5	9.5	11.5
Enzyme		0.06 g/l	0.06 g/l	0.02 g/l	0.10 g/l	0.06 g/l	0.06 g/l
Frequency Factor		1.58%					
Shear Stress		N/A					
SIMULATION PARAMETERS							
Swelling	Diffusion Coefficient, D	3.0·10 ⁻¹⁰ m ² /s	4.0·10 ⁻¹⁰ m ² /s	4.0·10 ⁻¹⁰ m ² /s	4.0·10 ⁻¹⁰ m ² /s	2.5·10 ⁻¹⁰ m ² /s	9.0·10 ⁻¹⁰ m ² /s
	Flory-Huggins Parameter, X	0.9	0.8	0.8	0.8	0.8	0.0
	Polymer Chains Per Unit Volume, N	5.5·10 ²⁶ m ⁻³					
	Volume Per Solvent Molecule, Ω	3·10 ⁻²⁹ m ³					
	Equilibrium Thickness, <i>h_{max}</i>	0.410 mm	0.703 mm	0.703 mm	0.703 mm	0.445 mm	0.822 mm
Lag Time		13.05 min	3.14 min	8.45 min	0.41 min	0.93 min	5.92 min
Shear Stress Removal Rate		-24.28 μm/min	-69.42 μm/min	-31.06 μm/min	-95.66 μm/min	-19.20 μm/min	-154.65 μm/min
Soil Dissolution Removal Rate		-2.84 μm/min	-9.63 μm/min	-7.82 μm/min	-12.19 μm/min	-7.69 μm/min	-22.93 μm/min

487

488

489 Simulations showed good agreement with real data in 4 (#1, #2, #4 and #6) of the 6 cases. The
 490 algorithm was able to make close predictions under circumstances where cleaning conditions in
 491 reality were relatively strong, that is, mid or high levels of enzymes, temperature and pH. The
 492 other two cases (#3 and #5) not showing an accurate prediction belonged to scenarios where the
 493 cleaning rates were the lowest ones observed. As the frequency factor (f) was established at
 494 1.58%, the main mechanism for cleaning was soil dissolution. This means removal occurred most
 495 of the time by the only action of the enzyme as the application of an external mechanical action
 496 was not so frequent. Therefore, main distortions to predictions were introduced by the soil
 497 dissolution removal rate (SD) term. For cases #3 and #5, to produce similar profiles between real
 498 and simulated data, soil dissolution rates should have been established around -0.90 (vs. -7.82
 499 estimated) μ m/min and -2.00 μ m/min (vs. -7.69 estimated). Raw data inputted to generate the
 500 statistical soil dissolution removal rate model showed no smaller value than -3.90 μ m/min. This

value corresponded to the experimental case at lowest temperature (30°C), pH (9.5) and enzyme level (0.02 g/l) in the sFDG. As a consequence, the statistical model built will never be able to predict such low removal rates within the levels studied.

Negative values shown at early times on some experimental data (i.e. #1) corresponds to the initial wetting phenomenon on the front of the camera lens. This distorted the initial data collected by obscuring the images. Therefore, SRI estimated was found to be slightly lower than 0%. This deviation was checked to be negligible once the presence of drops or moisture on the camera kit stabilised and the variation of color due to the external factors disappeared.

Main differences between sFDG and ADW set-ups are summarised in **Table 6**. To explain the divergences observed, different enzyme deposition levels on the soil tile between the two methods are suggested. In the ADW and at low concentrations, the enzyme molecules could struggle to bind to the soil surface. The low availability of enzyme combined with the vertical placement of the tile plus a fast solution renewal means that less enzyme molecules are deposited and thus the hydrolysis of the sample is reduced. In sFDG tests, the horizontal placement of the soil immersed in the wash solution with a slow renewal of it offers advantages for this enzyme deposition. At higher concentrations, the higher number of enzyme molecules could compensate the disadvantages previously observed in the ADW and more molecules could bind the soil surface per unit time thus increasing the soil dissolution rate as observed. In the sFDG, the increase in the number of enzyme molecules could increase the soil dissolution rate as well, however, due to the poor solution renewal the transport of hydrolysed soil material to the bulk solution could be done much slower, therefore reducing or making the previous divergences negligible.

Table 6. Main differences between sFDG and Full-Scale experimental set-ups.

	sFDG	FULL-SCALE
Position of the tile	Horizontal	Vertical
Tile completely sunk	Yes	No
Wash solution renewal	Slow	Fast

Wash solution renewal relates to the frequency action. A same frequency factor value can be achieved through multiple ways. Thus, for example, a frequency value of 50% is typically achieved in the sFDG when the nozzle is sit on the sample for 30 seconds at intervals of 1 minute. In an ADW this could be achieved if a jet is hitting a sample during 0.75 seconds in a typical rotation rate of 1.5 seconds. Therefore, when we discuss about wash solution renewal in this case, we refer to how often that mechanical action occurs and not the average time indicated by the frequency factor. The integrated model represented by **Eq. 1** also takes this into consideration.

Another source of divergences can be the assumption of a full correlation between the variation of the soil thickness and the changes in color. Despite both techniques are able to show the same cleaning patterns, it might occur that the removal of a soil layer does not completely corresponds to the equivalent %SRI change. A deeper follow-up is therefore suggested on this point to clarify in more detail the link between the percentage of removal estimated with the sFDG and the %SRI change observed via an image analysis system.

Finally, the final decay stage of the cleaning process is also missing in the simulation. This stage relates to the final adhesive removal of the soil sample (soil layers that are attached to the substrate). As these soils that detach layer by layer break cohesively, it means these adhesive forces are higher, thus more energy is required for the removal. If the cleaning conditions are maintained constant through the wash cycle (as this is the case) this translates into a larger time to remove the same amount of soil and therefore into the reduction of the speed of removal. This is lately shown as a decrease on the slope of the experimental data. The phenomenon explained can be observed in **Figures 7.2** and **7.4**. The model replicates the real data with good accuracy until the SRI reaches 70% approximately. From this point on, the removal rate decreases for real data while for simulated data the removal rate remains invariant as it is assumed a constant removal rate (linear) throughout the process.

Figure 8 represents the differences in removal rates observed between real and simulated data. The graph allows to easily recognise which conditions need to be analysed in more detailed to enhance the quality of the model proposed. A contour line with a negative value refers to

experimental conditions where the model underpredicts the real data obtained, while those lines with a positive value corresponds to an overprediction of the model.

Areas with higher divergences are found at the limits of the levels set experimentally for the different factors. These areas are less robust statistically due to the lower number of data collected. Also, they are the ones where the divergences between experimental techniques are higher as already commented. At the highest levels set, the model slightly underpredicts the results, though the deviations are not as high as the ones observed for the lowest levels tested, where significant overpredictions can be seen. The best correlations are given at pH values between 10.5 and 11 for mainly all the ranges of temperature and enzyme levels studied.

5. Conclusions

This paper presented the first effort to predict the removal of protein-based soils in automatic dishwashers. An integrated model combining the mechanical action from the appliance and the different removal mechanisms occurring on a typical soil was introduced.

The model has shown to be a valid approach though it still requires a more refined approach to make it more accurate. Difficulties arose when assuming a complete correlation from the thickness data obtained via de sFDG and the SRI data estimated via image analysis. Future work would have to focused on how these techniques correlate by studying in detail the link between the removal of a soil layer with the change in colour produced. Data shown in these work suggests that the correlation exists as similar trends were clearly captured by the two techniques. Also, the differences between the different set-ups must also be considered. The benefits of this methodology is that enables different profiles over time of the cleaning factors used as inputs. This feature is essential to mimic temperature, pH or enzyme level changes during a typical wash cycle.

The use of dynamic models is a tool with high potential in the understanding and the analysis of the performance of different formulations. The inclusion of time as a factor multiplies the information gathered and allows better and faster decisions to be made. By evaluating not only

the end cleaning point of a specific formulation, but also the evolution of the soil over time, it is possible to know where a formulation performs at its best.

Acknowledgements

This research was funded by the Engineering and Physical Science Research Council (EPSRC, Grant No. EP/G036713/1) and industrially sponsored by Procter & Gamble. The authors would like to thank Zayeed Alam and Carlos Amador for their help and useful discussion.

References

- Aehle, W., 2007. *Enzymes in Industry: Production and Applications*, Third Ed. ed. Wiley-VCH Verlag GmbH & Co. KGaA, Weinheim, Germany. doi:10.1002/9783527617098
- AHAM, 1992. AHAM DW-1: Household Electric Dishwashers by Association of Home Appliance Manufacturers. United States of America.
- Ali, A., de'Ath, D., Gibson, D., Parkin, J., Alam, Z., Ward, G., Wilson, D.I., 2015. Development of a "millimanipulation" device to study the removal of soft solid fouling layers from solid substrates and its application to cooked lard deposits. *Food Bioprod. Process.* 93, 256–268. doi:10.1016/j.fbp.2014.09.001
- Berkholz, P., Stamminger, R., Wnuk, G., Owens, J., Bernarde, S., 2010. Manual dishwashing habits: an empirical analysis of UK consumers. *Int. J. Consum. Stud.* 34, 235–242. doi:10.1111/j.1470-6431.2009.00840.x
- Bezerra, M.A., Santelli, R.E., Oliveira, E.P., Villar, L.S., Escaleira, L.A., 2008. Response surface methodology (RSM) as a tool for optimization in analytical chemistry. *Talanta* 76, 965–977. doi:10.1016/j.talanta.2008.05.019
- Bird, M.R., Fryer, P.J., 1991. An experimental study of the cleaning of surfaces fouled by whey proteins. *Food Bioprod. Process. Trans. Inst. Chem. Eng. Part C* 69, 13–21.
- Christian, G.K., Fryer, P.J., 2006. The effect of pulsing cleaning chemicals on the cleaning of whey protein deposits. *Food Bioprod. Process.* 84, 320–328. doi:10.1205/fbp06039
- Cole, P.A., Asteriadou, K., Robbins, P.T., Owen, E.G., Montague, G.A., Fryer, P.J., 2010. Comparison of cleaning of toothpaste from surfaces and pilot scale pipework. *Food Bioprod. Process.* 88, 392–400. doi:10.1016/j.fbp.2010.08.008
- Denmat, M., Anton, M., Gandemer, G., 1999. Protein Denaturation and Emulsifying Properties of Plasma and Granules of Egg Yolk as Related to Heat Treatment. *J. Food Sci.* 64, 194–197. doi:10.1111/j.1365-2621.1999.tb15863.x

- DuPont, 2012. US consumer dishwashing study [WWW Document]. URL <http://fhc.biosciences.dupont.com/consumer-trends/consumer-studies/us-consumer-dishwashing-study/> (accessed 12.5.14).
- Fryer, P.J., Christian, G.K., Liu, W., 2006. How hygiene happens: physics and chemistry of cleaning. *Soc. Dairy Technol.* 59, 76–84. doi:10.1111/j.1471-0307.2006.00249.x
- Geladi, P., Kowalski, B., 1986. Partial least-squares regression: a tutorial. *Anal. Chim. Acta.*
- Goode, K.R., Asteriadou, K., Fryer, P.J., Picksley, M., Robbins, P.T., 2010. Characterising the cleaning mechanisms of yeast and the implications for Cleaning in Place (CIP). *Food Bioprod. Process.* 88, 365–374. doi:10.1016/j.fbp.2010.08.005
- Gordon, P.W., Brooker, A.D.M., Chew, Y.M.J., Letzelter, N., York, D.W., Wilson, D.I., 2012. Elucidating enzyme-based cleaning of protein soils (gelatine and egg yolk) using a scanning fluid dynamic gauge. *Chem. Eng. Res. Des.* 90, 162–171. doi:10.1016/j.cherd.2011.07.007
- Gordon, P.W., Brooker, A.D.M., Chew, Y.M.J., Wilson, D.I., York, D.W., 2010a. A scanning fluid dynamic gauging technique for probing surface layers. *Meas. Sci. Technol.* 21, 085103. doi:10.1088/0957-0233/21/8/085103
- Gordon, P.W., Brooker, A.D.M., Chew, Y.M.J., Wilson, D.I., York, D.W., 2010b. Studies into the swelling of gelatine films using a scanning fluid dynamic gauge. *Food Bioprod. Process.* 88, 357–364. doi:10.1016/j.fbp.2010.08.012
- Jin, L., Li, D., 2007. A switching vector median filter based on the CIELAB color space for color image restoration. *Signal Processing* 87, 1345–1354. doi:10.1016/j.sigpro.2006.11.008
- Liu, W., Aziz, N., Zhang, Z., Fryer, P., 2005. Quantification of the cleaning of egg albumin deposits using micromanipulation and direct observation techniques. *J. Food Eng.* 78, 217–224. doi:10.1016/j.jfoodeng.2005.09.019
- Liu, W., Christian, G.K., Zhang, Z., Fryer, P.J., 2002. Development and use of a micromanipulation technique for measuring the force required to disrupt and remove fouling deposits. *Inst. Chem. Eng.* 80 Part C.
- Liu, W., Christian, G.K., Zhang, Z., Fryer, P.J., 2006a. Direct measurement of the force required to disrupt and remove fouling deposits of whey protein concentrate. *Int. Dairy J.* 16, 164–172. doi:10.1016/j.idairyj.2005.02.008
- Liu, W., Fryer, P.J., Zhang, Z., Zhao, Q., Liu, Y., 2006b. Identification of cohesive and adhesive effects in the cleaning of food fouling deposits. *Innov. Food Sci. Emerg. Technol.* 7, 263–269. doi:10.1016/j.ifset.2006.02.006
- Liu, W., Zhang, Z., Fryer, P., 2006c. Identification and modelling of different removal modes in the cleaning of a model food deposit. *Chem. Eng. Sci.* 61, 7528–7534. doi:10.1016/j.ces.2006.08.045

- 661 Mine, Y., Zhang, H., 2013. *Biochemistry of Foods*, Third Ed. ed, Biochemistry of Foods. Elsevier.
662 doi:10.1016/B978-0-08-091809-9.00005-4
- 663 Neiditch, O.W., Mills, K.L., Gladstone, G., Brothers, L., 1980. The Stain Removal Index (SRI): A
664 New Reflectometer Method for Measuring and Reporting Stain Removal Effectiveness. *J.*
665 *Am. Oil Chem. Soc.* 57, 426–429. doi:10.1007/BF02678931
- 666 Olsen, H.S., Falholt, P., 1998. The role of enzymes in modern detergency. *J. Surfactants Deterg.*
667 1, 555–567. doi:10.1007/s11743-998-0058-7
- 668 Othman, A., Asteriadou, K., Robbins, P., Fryer, P., 2010. Cleaning of sweet condensed milk
669 deposits on a stainless steel surface. *Fouling Clean. Food Process.*
- 670 Pérez-Mohedano, R., Letzelter, N., Amador, C., VanderRoest, C.T., Bakalis, S., 2015a. Positron
671 Emission Particle Tracking (PEPT) for the analysis of water motion in a domestic
672 dishwasher. *Chem. Eng. J.* 259, 724–736. doi:10.1016/j.cej.2014.08.033
- 673 Pérez-Mohedano, R., Letzelter, N., Bakalis, S., 2015b. Development of a swelling-removal model
674 for the scanning fluid dynamic gauge. *Food Bioprod. Process.* 93, 269–282.
675 doi:10.1016/j.fbp.2014.10.001
- 676 Pérez-Mohedano, R., Letzelter, N., Bakalis, S., 2016. Swelling and hydration studies on egg yolk
677 samples via scanning fluid dynamic gauge and gravimetric tests. *J. Food Eng.* 169, 101–
678 113. doi:10.1016/j.jfoodeng.2015.08.014
- 679 Tomlinson, A., Carnali, J., 2007. A Review of Key Ingredients Used in Past and Present Auto-
680 Dishwashing Formulations and the Physico-Chemical Processes They Facilitate, in:
681 Johansson, I., Somasundaran, P. (Eds.), *Handbook for Cleaning/Decontamination of*
682 *Surfaces*. Elsevier B.V, pp. 197–255.
- 683 Tsutsui, T., 1988. Functional Properties of Heat-Treated Egg Yolk Low Density Lipoprotein. *J.*
684 *Food Sci.* 53, 1103–1106.
- 685 Tuladhar, T.R., Paterson, W.R., Macleod, N., Wilson, D.I., 2000. Development of a novel
686 non-contact proximity gauge for thickness measurement of soft deposits and its application
687 in fouling studies. *Can. J. Chem. Eng.* 78, 935–947. doi:10.1002/cjce.5450780511
- 688 Tuladhar, T.R., Paterson, W.R., Wilson, D.I., 2002. Thermal Conductivity of Whey Protein Films
689 Undergoing Swelling. *Food Bioprod. Process.* 80, 332–339.
690 doi:10.1205/096030802321154862
- 691 Wang, T., Davidson, J.F., Wilson, D.I., 2013a. Effect of surfactant on flow patterns and draining
692 films created by a static horizontal liquid jet impinging on a vertical surface at low flow rates.
693 *Chem. Eng. Sci.* 88, 79–94. doi:10.1016/j.ces.2012.11.009
- 694 Wang, T., Davidson, J.F., Wilson, D.I., 2014. Flow patterns and cleaning behaviour of horizontal
695 liquid jets impinging on angled walls. *Food Bioprod. Process.* 93, 333–342.
696 doi:10.1016/j.fbp.2014.09.006

- Wang, T., Faria, D., Stevens, L.J., Tan, J.S.C., Davidson, J.F., Wilson, D.I., 2013b. Flow patterns and draining films created by horizontal and inclined coherent water jets impinging on vertical walls. *Chem. Eng. Sci.* 102, 585–601. doi:10.1016/j.ces.2013.08.054
- Wilson, D.I., 2005. Challenges in Cleaning: Recent Developments and Future Prospects. *Heat Transf. Eng.* 26, 51–59. doi:10.1080/01457630590890175
- Wilson, D.I., Atkinson, P., Köhler, H., Mauermann, M., Stoye, H., Suddaby, K., Wang, T., Davidson, J.F., Majschak, J.P., 2014. Cleaning of soft-solid soil layers on vertical and horizontal surfaces by stationary coherent impinging liquid jets. *Chem. Eng. Sci.* 109, 183–196. doi:10.1016/j.ces.2014.01.034
- Wilson, D.I., Le, B.L., Dao, H.D.A., Lai, K.Y., Morison, K.R., Davidson, J.F., 2012. Surface flow and drainage films created by horizontal impinging liquid jets. *Chem. Eng. Sci.* 68, 449–460. doi:10.1016/j.ces.2011.10.003
- Wold, H., 1985. Partial least squares. *Encycl. Stat. Sci.* 1–10.

Appendix. Time in ‘vision area’ (t_{vis}), Time impacting items (T_{impact}) and Impact Length (L_{impact}) per spray are rotation.

Let there be a circular item of diameter ‘ D_{item} ’ located vertically at coordinates (x_{item} , y_{item} , z_{item}) with a separation from the front item ‘ d ’. Let there be also a nozzle located at a radial distance R_{NZ} , a height z_{NL} and rotating from an axis of rotation at (0,0, z_{NL}) coordinates. The angles at which the nozzle enters (β_{in}) and exits (β_{out}) the defined vision area can be calculated as follow:

$$\beta_{in} = \arcsin\left(\frac{y_{item} - d}{R_{NZ}}\right) \quad (A.1)$$

$$\beta_{out} = \arcsin\left(\frac{y_{item}}{R_{NZ}}\right) \quad (A.2)$$

Given a rotational speed of the spray arm ω ($\omega = \frac{d\beta}{dt}$), the time the nozzle (jet) is travelling in the ‘vision area’ is given by:

$$t_{vis} = \frac{|\beta_{out} - \beta_{in}|}{\omega} \quad (A.3)$$

In between those angles, the path followed by the nozzle is given by:

$$x_{NZ} = R_{NZ} \cdot \cos(\beta_{NZ}) \quad (A.4)$$

$$y_{NZ} = R_{NZ} \cdot \sin(\beta_{NZ}) \quad (A.5)$$

Where: $\beta_{in} > \beta > \beta_{out}$

A time value can also be assigned for each of the nozzle locations if the rotational speed ω is known.

The Cartesian components of the direction vector characterising the jet path are calculated as follow:

$$\text{x-direction: } (dir)_x = 1 \quad (A.6)$$

$$\text{y-direction: } (dir)_y = (dir)_x \cdot tg(\theta_{jet}) \quad (A.7)$$

$$\text{z-direction: } (dir)_z = \sqrt{(dir)_x^2 + (dir)_y^2} \cdot tg(\rho_{jet}) \quad (A.8)$$

With those parameters, the impact locations on the x-z plane formed by the analysed item are given by:

$$x_{item} - \frac{D_{item}}{2} < x_{impact}(t) = \frac{(y_{item} - y_{NZ}(t))}{(dir)_y} \cdot (dir)_x + x_{NZ}(t) < x_{item} + \frac{D_{item}}{2} \quad (A.9)$$

$$z_{item} - D_{item} < z_{impact}(t) = \frac{(y_{item} - y_{NZ}(t))}{(dir)_y} \cdot (dir)_z + z_{NZ}(t) < z_{item} \quad (A.10)$$

The times at which the first and last impact locations within the boundaries of the analysed item occur indicate the total impact time (T_{impact}). The sum of the distance between consecutive impact locations within the analysed item edges gives the length coverage by the jet (L_{impact}). The calculus is equivalent for a rectangular item by just changing the boundaries at which the impact occurs in eq. 9 and eq. 10.

Nomenclature

D	diffusion coefficient
f	frequency function
h	thickness
h_{\max}	thickness at equilibrium
L_{impact}	length covered by impacting jet on analysed item
N	number of polymer chains per unit volume
R^2	goodness of fit
R_{nz}	radial position of nozzle
S	swelling function
SD	soil dissolution function
SS	shear stress function
t	time
t_{vis}	nozzle time in vision area
T_{impact}	duration a jet is impacting the analysed item per rotation
x,y,z	cartesian coordinates

Greek symbols

β_{in}	angular position at entrance in vision area
β_{out}	angular position at exit of vision area
θ_{jet}	theta angle – angle in the x-y plane (plan view)
ρ_{jet}	rho angle - angle between the x-y plane and z-axis (front view)
χ	Flory-Huggins parameter
Ω	volume of a solvent molecule (water)
ω	rotational speed of the spray arm

Abbreviations

ADW	automatic dishwasher
CFT	centre for testmaterials
CIE	commission internationale de l'eclairage (commission on illumination)

CIP	cleaning in place
FDG	fluid dynamic gauging
HDL	high density lipoproteins
L*a*b	color space (CIE 1976)
LDL	low density lipoproteins
PEPT	positron emission particle tracking
PLS	partial least squares
RGB	color space (red green blue)
RS	response surface
sFDG	scanning fluid dynamic gauging
SRI	stain removal index

Figure Captions

Figure 1. Schematic of the integrated model approach to simulate cleaning profiles in an ADW.

Figure 2. Schematic of the experimental set-up for ADW tests. A – Plan view. B – Side view. Coordinates (x,y,z) of the 4 corners defining the area occupied by the soil tile: 1 (-35, 245, 180); 2 (-35, 245, 240); 3 (-35, 145, 240); 4 (-35, 145, 180). Origin of the reference system was located at the bottom in the centre of the ADW.

Figure 3. Schematic representation of polar angles to define the 3D trajectory of a water jet.

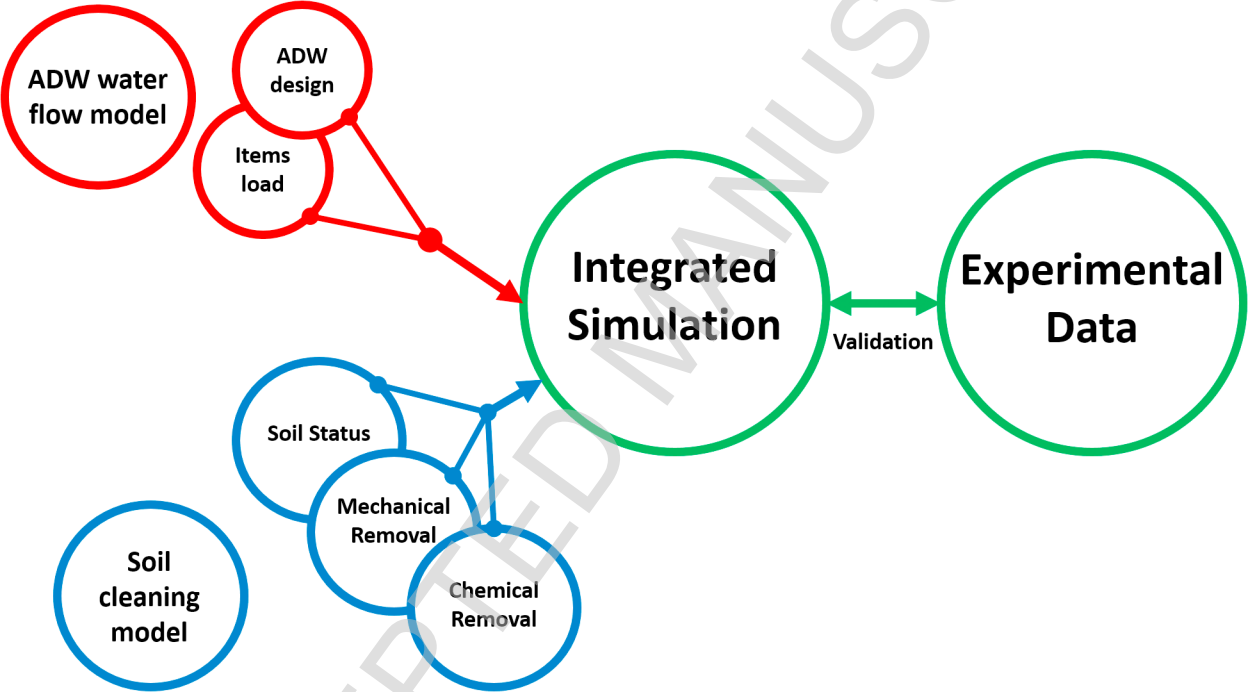
Figure 4. Plan view of a schematic of different angles covered by two nozzles placed at different radial distances. Red and green dotted lines show the trajectories considered. β angles represent the angles formed between the position at which a nozzle enters the 'vision area', the origin and the soiled item.

Figure 5. Normalized effect over time of the different significant factors remaining.

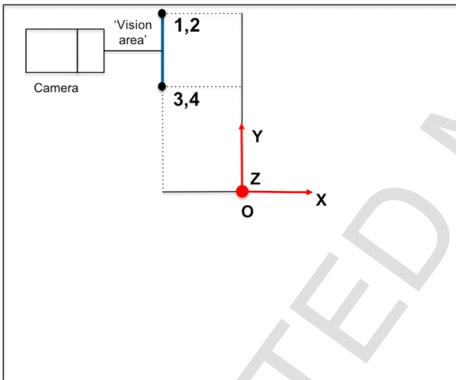
Figure 6. Actual by predicted plots for soil dissolution removal rate (A), shear stress removal rate (B) and lag time (C) response surface models. Dotted red lines represent the confidence interval ($p=0.05$) and blue line represents the average among all values inputted.

Figure 7. Experimental and simulation results for the six different cases considered. Experimental conditions and simulation parameters are shown in **Table 5**. Blue line represents experimental data while red line corresponds to simulation results. Blue shadow indicates the standard error shown experimentally.

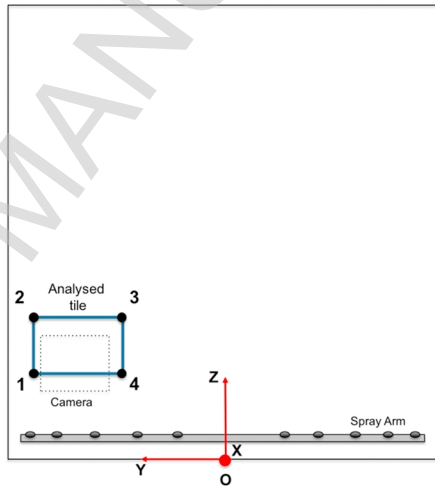
Figure 8. Contour plots to illustrate differences between simulated and real data. A – Temperature ($^{\circ}\text{C}$) vs Enzyme (g); B – Temperature ($^{\circ}\text{C}$) vs pH; C – pH vs Enzyme (g).



A
PLAN VIEW

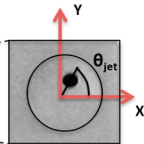
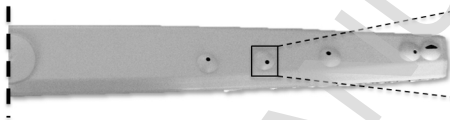
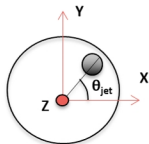


B
SIDE VIEW



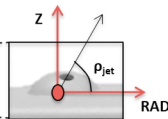
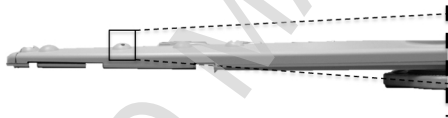
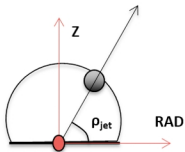
Nozzle design

Plan view

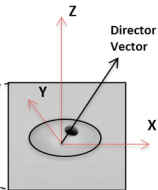
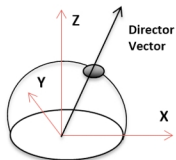


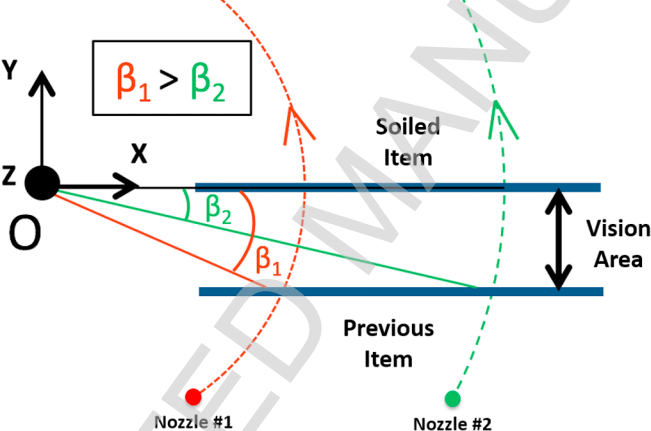
*Rotated 90°

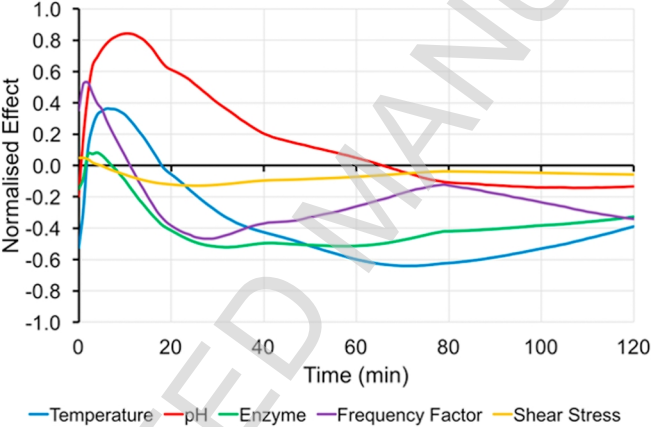
Front view



3D

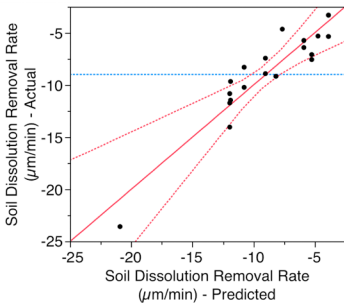






A

Soil Dissolution (SD)

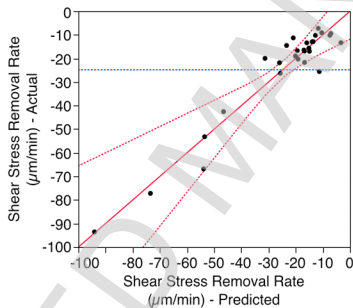


$$R^2 = 0.862$$

$$R^2 \text{ Adj.} = 0.695$$

B

Shear Stress (SS)

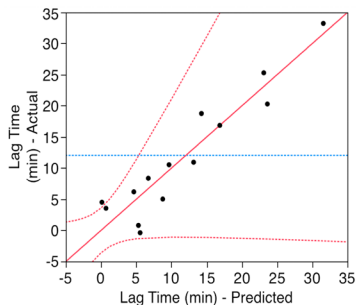


$$R^2 = 0.848$$

$$R^2 \text{ Adj.} = 0.718$$

C

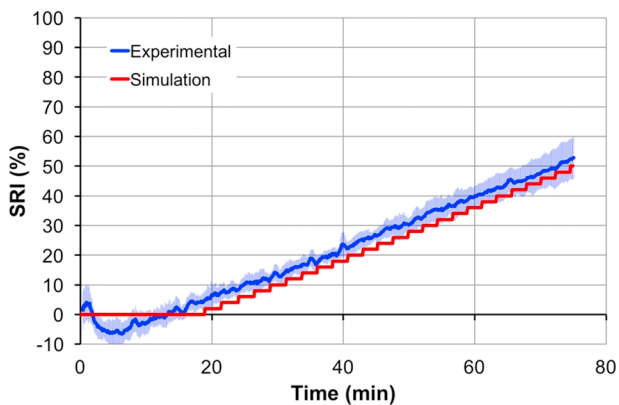
Lag time



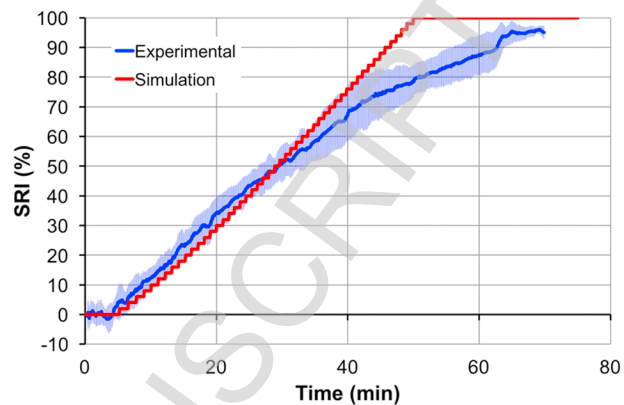
$$R^2 = 0.878$$

$$R^2 \text{ Adj.} = 0.633$$

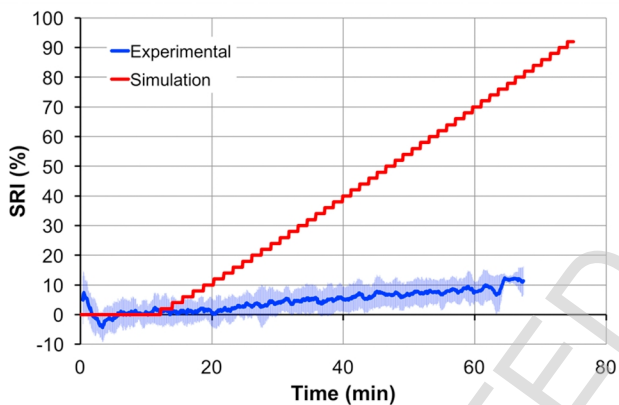
1



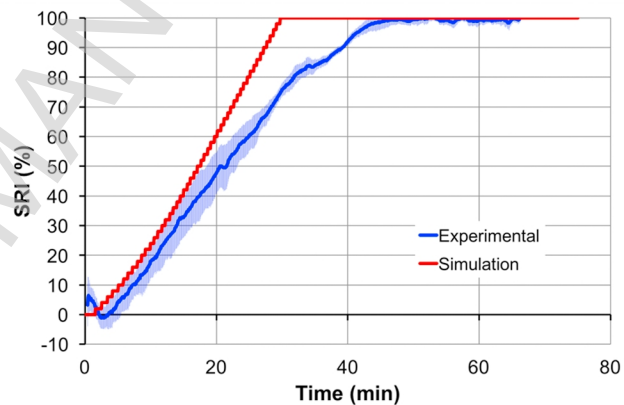
2



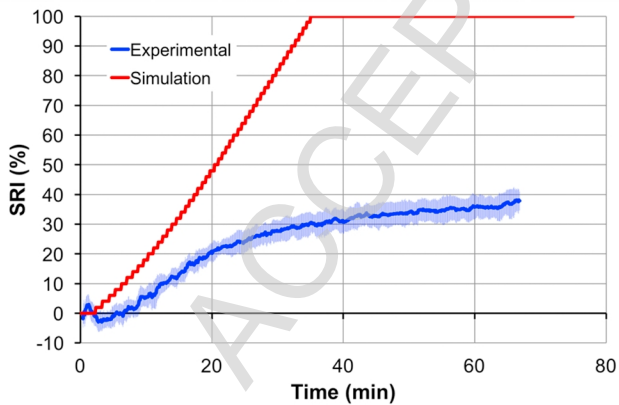
3



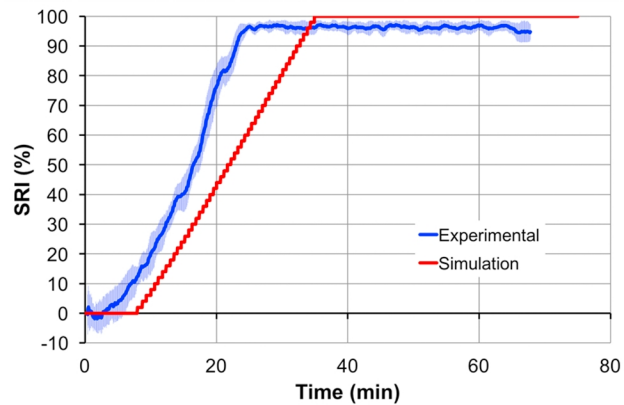
4

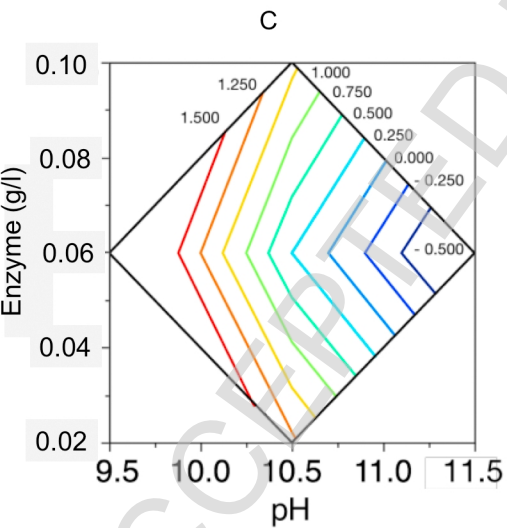
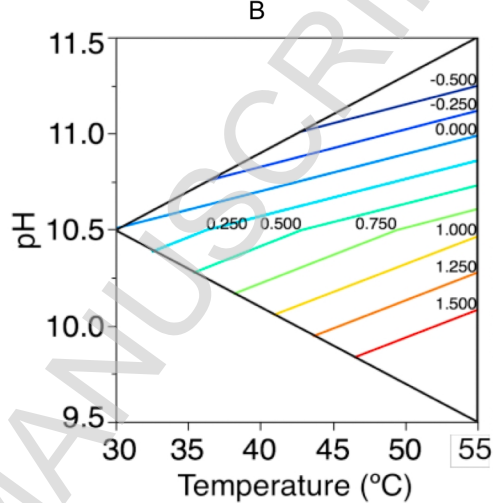
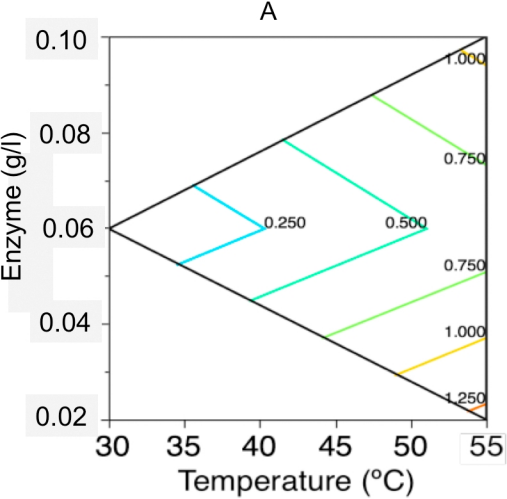


5



6





Difference Simulated vs Real

